June 2010 ISSN : 0974 - 7486 Volume 6 Issue 2

Materials Science

Trade Science Inc.

An Indian Journal

Full Paper

MSAIJ, 6(2), 2010 [125-131]

Microstructure control of HIPed inconel 718 alloy

N.El-Bagoury[1,2]*, M.Ramadan[1,3], M.Waly[1], K.Ogi[4]

[1]Casting Dept., Central Metallurgical Research and Development Institute (CMRDI), P.O. Box 87 Helwan, Cairo, (EGYPT)

[2]Chemistry Dept. Faculty of Science, TAIF University, P.O. Box 888, El-Haweyah, El-Taij, (KINGDOM OF SAUDI ARABIA)

[3]Materials Engineering, Faculty of Engineering, HAEL University, P.O. Box 2440 Hail, (KINGDOM OF SAUDI ARABIA)

[4]Department of Materials Science & Engineering, Kyushu University, 744 Motooka, Nishi-Ku, Fukuoka, 819-0395, (JAPAN)

E-mail : nader_elbagoury@yahoo.com

Received: 7th March, 2010 ; Accepted: 17th March, 2010

ABSTRACT

The influence of solution and aging heat treatment processes on microstructure of Hipped Inconel 718 (IN718) alloy has been investigated. Conventional solution treatment (CST) at 1273K for 1h precipitates a thin film of δ phase at the grain boundaries of γ matrix. However, after solution at 1440K for 3h long (modified solution), the precipitates of δ phase entirely eradicate from the microstructure. Small colonies of needle-like δ phase start to appear with aging at 1023K for 4h, after CST. Prolonging the aging time to 50h, these colonies enlarge in size and spread in the matrix. XRD and TEM observations were used to identify the precipitation of hard γ″ and γ′ phases. The changing in hardness measurements was evidence about the precipitation of these hard phases. CST has higher rate to increase in hardness with aging time comparing to modified solution specimens.

KEYWORDS

Ni base superalloys;
Inconel 718;
Solution and aging treatment;
Microstructure;
Hardness.

INTRODUCTION

INCONEL 718 alloy is one of the most highly utilized Ni-Base Superalloy and is a commonly used material for manufacturing of turbine and aerospace components. This alloy is age-hardened by the homogenously precipitated of γ″ and γ′ phases, which allow the alloy to have a high strength at moderate temperatures and good creep and fatigue resistance[1-4].

Transmission electron microscope (TEM) could be used to identify the superlattice spots diffraction of the γ′ and γ″ precipitates throughout morphology and orientation relationship of these precipitates in this alloy[5].

The strengthening phase in IN718 alloy that precipitated after aging treatment is the metastable body centered tetragonal Ni_3Nb (DO_{22}) γ″ phase[6-8]. This phase is long disc-shaped and lies parallel to the {100} planes of the matrix[9]. Moreover, the ordered face centered cubic Ni_3 (Al, Ti), ($L1_2$) γ′ phase is precipitated in a small amount as a fine dispersion, of quasi-spherical particles which are coherent with γ matrix[10].

Additionally, δ phase with orthorhombic (DO_a) can precipitate at 923K and above and this is the major consideration. The plate-like δ phase is harmful for the mechanical properties of IN718 alloy[11-13]. Most of Ni base superalloys strengthened by precipitations of γ″ phase are prone to δ phase, which occurs during processing or service[14].

The heat treatment scheme of IN718 alloy is divided into solid solution and aging treatment. Solution treatment process dissolves the eutectic phases Ni_2Nb (Laves) phase, in addition to reducing the chemical segregation of the alloying elements[15].

This research aims at studying the effect of solution and aging treatment conditions on the microstructure of IN718 alloy. The precipitations of γ'', γ' phases and elimination of δ phase to improve the final mechanical properties, represented by hardness property, of IN718 alloy.

EXPERIMENTAL

Materials and chemical composition

The nominal chemical composition of standard IN718 alloy used in this study is presented in TABLE 1. This alloy was melted by a high frequency vacuum induction furnace then cast into Y-block type samples under vacuum. Fine and coarse grain samples were prepared by pouring the melt into preheated (1273K) ceramic mold at 1633 and 1708K, respectively. After casting, the samples were HIPed at 1440K for 4h under pressure of 143MPa to eliminate the shrinkage and gas porosity formed during casting.

Heat treatment conditions

Two conditions of solution treatment process have been carried out. The first solution treatment was the conventional one at 1273k for 1h[16-18], and the other one was the modified solution treatment at 1440K for 3h, both were followed by water quenching.

After solution treatment, the aging processes were accomplished at two temperatures of 953 and 1023K with various aging time ranging from 2 up to 150h.

Metallographic microstructure identification

All samples were sectioned and polished, using conventional metallographic preparation techniques. Shimadzu EPMA-1600 was used to investigate the precipitation of δ phase. Both Super Back Scattered Electron (SBSE) and Reflected Electron (RE) images were very helpful to recognize and differentiate between various phases such as Ni_2Nb (laves), NbC and Delta phase.

X-ray diffraction (XRD) analyses were carried out with a (θ-2θ) Rigaku (Rint 2100) diffractometer by using Co-Kα radiation (λ = 1.788965A°) and working in the following conditions: 50kV as acceleration voltage and 50 mA for the current.

Selected samples were prepared for transmission electron microscope. TEM examinations were carried out with JEOL Electron Microscope (JEM-1000). The latter was operated at 1000 kV and equipped with a tilt rotation probe holder. After the aging treatment, the samples were mechanically ground to ~80μm thickness, then electro-polished using a Struers twin-jet at room temperature in a bath containing chemical solution of 70% $C_2H_5OC_2H_5$, 20% C_2H_5OH and 10% $HClO_4$, under 15V.

Hardness measurements

Hardness was measured using MNK-H1 Akashi Hardness Tester Machine (Akashi Co. Ltd.) under a load of 30Kg. The mean value over ten measurements was evaluated.

RESULTS AND DISCUSSION

Structure of treated specimens and δ phase precipitation

Solution treatments

The solution heat treatment is intended to dissolve both γ'' and γ' that formed during the cooling during solidification and that remained after HIPing process. Additionally solution treatments reduce the degree of chemical segregation due to the partitioning of some of alloying elements to the dendrite core and interdendritic regions.

By using EPMA, the microstructure of the solution treated IN718 alloy has been investigated. Figure 1 shows the microstructure of the conventional solution (1273K for 1h) specimen, which consists of primary γ matrix, eutectic (γ+NbC) and δ phase. This δ phase

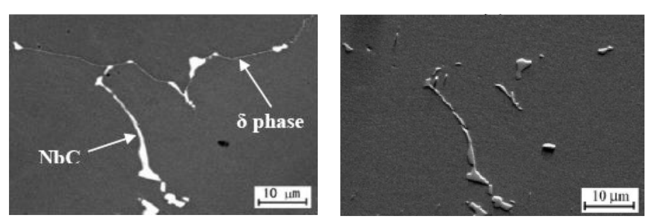

(a) (b)

Figure 1 : Microstructure of standard solution specimen, (a) SBSE and (b) RE images

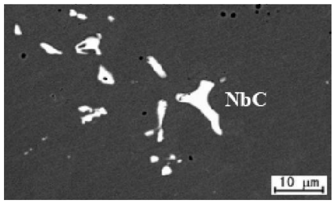

Figure 2 : Microstructure of modified solution specimen

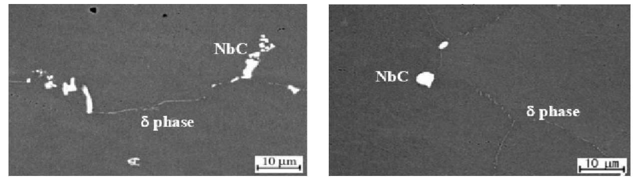

(a) (b)

Figure 3 : Microstructure of CST specimen aged at 953K

precipitates as a thin film at the grain boundaries of γ matrix. Also figure 1(a) and 1(b), show the differentiation between NbC and δ phase. These phases have the same white color in SBSE image, but their hardness is different; therefore, the interpenetration between these white phases has been overcome due to their levels in RE image. As the NbC carbide has higher hardness values, it has the highest level in RE image in comparison with δ phase, as shown in Figure 1(b). Saied Azadian, et al.[19] found that the δ phase precipitates as a needle shape or as a thin film at the grain boundaries.

The microstructure of modified solution treated (1440K for 3h) specimen contains primary γ matrix and eutectic (γ+NbC). There is no presence of the precipitation of δ phase in this specimen's microstructure, as shown in figure 2.

Depending on the conditions of the heat treatment process, δ phase could be eliminated from the microstructure. The conventional solution treatment has lower temperature and shorter time in comparison with the modified solution one. The temperature level in conventional solution treatment (1273K) is very near to the temperature range for the precipitation of δ phase. The δ phase precipitates in the range between about 973 and 1273K. The rate of its precipitation is the highest at around 1173K. It normally precipitates by nucleation at grain boundaries followed by the growth of thin plates extending into the grains[17,19]. The formation of δ phase at 973K and above is a major consideration in limiting its use below this range of temperatures[20].

Because of its morphology, the δ phase does not contribute significantly to the hardening of the alloy. On the contrary, its presence implies a loss of hardenability due to the depletion of γ″. Moreover, its presence has been associated with an increased susceptibility to hot cracking[21].

Aging treatment

The microstructure of conventional solution treatment specimens, which aged at 953K for 4 and 50h, show the precipitations of δ phase at the grain boundaries figure 3(a) and 3(b). On the other hand, the microstructure of the modified solution specimen has no δ phase precipitation. Both SBSE and RE images illustrate the existence of NbC only in addition to the γ matrix, as shown in figure 4(a) and 4(b) after aging for 4 h and figure 4(c) for 50 h as well.

Aged microstructure at 1023k for 4h has precipitations of δ phase in the CST specimen, but not in the microstructure of modified solution specimen.

The absence of δ phase from the microstructure of modified solution treatment specimen is a positive landmark in decreasing the susceptibility for hot cracking of standard IN718 alloy[19]. Although the precipitation range for the δ phase is between about 923K and 1293K[22], the δ phase precipitation does not occur in the modified solution specimen after aging for 4h at 1023K. Prolonging the aging time to 50h at 1023K for the modified solution specimen has no evidence about the precipitation of δ phase in microstructure. While in figure 5, the microstructure of conventional solution treatment specimen that aged at 1023k for 50h contains thin δ phase film at the grain boundaries. The microstructure of these specimens illustrates the precipitation of some small size colonies of needle δ phase aged for 4h. After increasing aging time to 50h, these colonies of δ phase increase in size and extend into the grains, as shown in figure 5. This is an indication on the increase of the volume fraction of δ phase in the microstructure of conventional solution treatment specimens as aging time increases.

Figure 6 shows the line analysis for the plate-like δ phase at the grain boundaries of γ matrix of conventional solution treatment specimen[23]. The composition of these precipitates is enriched in Ni, Nb and Ti and depleted in Fe and Cr compared to the matrix composition.

Hardness changing after heat treatment

The HIPed standard IN718 alloy has been submit-

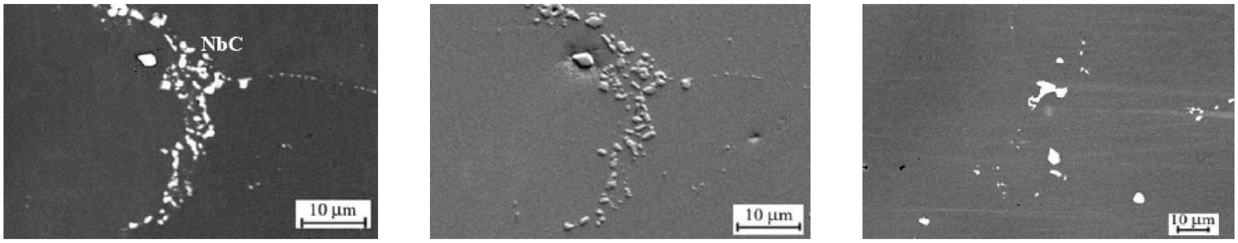

(a) (b) (c)

Figure 4 : Microstructure for the modified solution specimen aged at 953k for 4h (a) and (b) as well as for 50h (c)

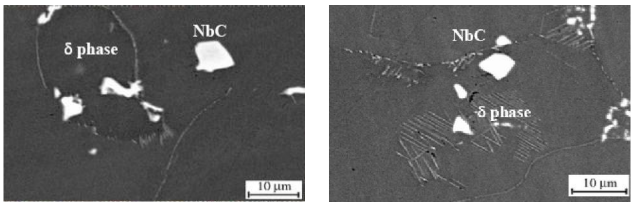

(a) (b)

Figure 5 : Microstructure of conventional solution treatment specimen aged at 1023k for 50h

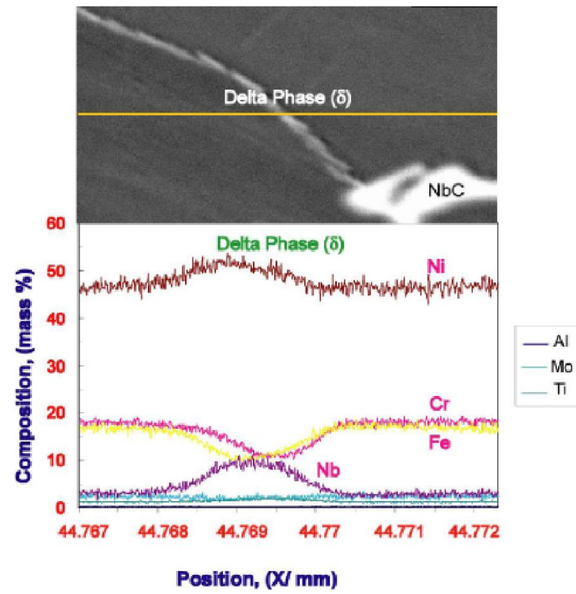

Figure 6 : Line analysis for delta phase in the specimen aged at 1023K for 100 h (conventional solution treatment)

ted to different heat treatment processes. At the beginning, two solution heat treatment processes (conventional and modified solution) have been carried out, and then followed by isothermal aging at two temperatures (953 and 1023K) for different durations of time.

Figure 7(a) and 7(b) show the changes in the hardness values as a function of the aging time at different temperatures. At 953K, figure 7(a), a rapid strengthening occurred for HIPed IN718 alloy in case of standard solution (1273K for 1 h) while in case of modified solution (1440K for 3 h) the hardness slowly changes with short durations of time starting from 0 up to 24h. The difference in hardness after 24 h between standard and modified solution treatments reaches about 100Hv where the hardness for standard solution specimen is 270Hv and for modified solution specimen is 170Hv. With the increase in aging time, the difference in hardness becomes smaller and both specimens take the same value of 390 Hv at 100 h. By prolonging the aging time from 100h to 150h, a slight increase in hardness values for the two specimens take place reaching about 399Hv.

Figure 7(b) shows the variation in hardness for standard and modified solution specimens after aging for different durations of time at 1023K. Both specimens of fine and coarse structures have the same hardness at different aging conditions for standard and modified solution specimens. The hardness of standard solution specimen reaches about 340Hv just after 10h while it was 230Hv at 953K after the same duration of time. The standard solution specimens harden more rapidly than modified ones, which need an incubation period to reach higher values of hardness. This incubation period for the hardening of modified solution specimens prolonged for 16h. Aging for 24 h was enough to increase the hardness of modified solution specimens to reach the same hardness values (385HV) for standard solution specimens while at 953K it takes 100h to get the same hardness. As the duration of aging increases to 50, 100 and 150h the hardness of modified solution specimens increase slightly to 395, 407 and 421Hv, respectively. After the same aging duration times, the hardness of standard solution specimens is lower than that for modified ones.

The hardness changes are related to the type of the precipitated phases, their volume fraction in the matrix, and their size.

Identification of γ and γ' precipitations

XRD examinations

The identification of precipitated phases by XRD

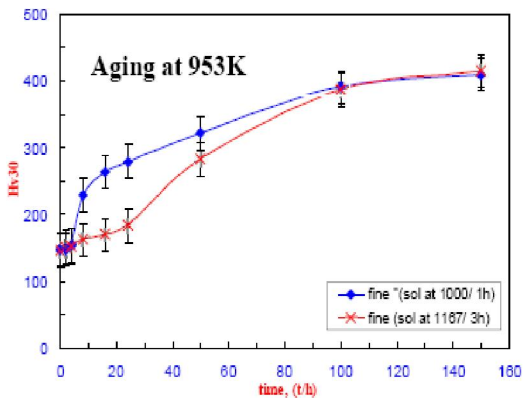

(a)

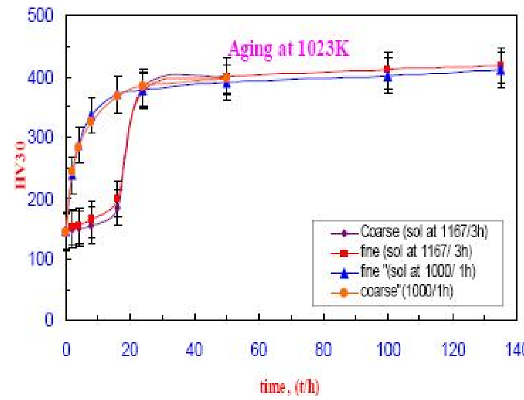

(b)

Figure 7 : Hardness measurements versus various aging heat treatment conditions, (a) at 953K and (b) at 1023K

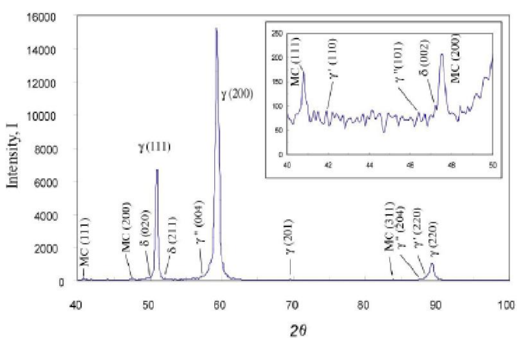

(a)

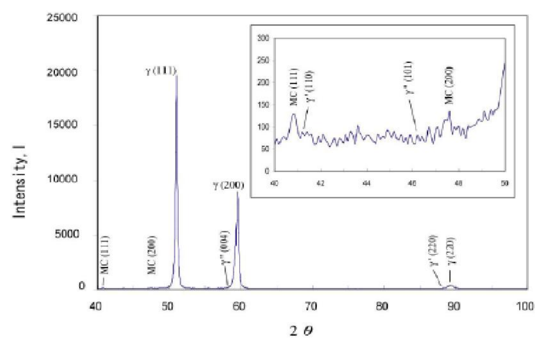

(b)

Figure 8 : X-ray diffraction pattern for aged specimen at 1023K for 4 h

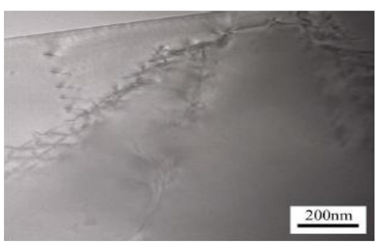

Figure 9 : Bright field micrograph of modified solution specimen

(a)

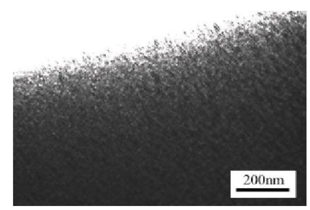

(b)

Figure 10 : Bright field micrograph for the modified solutionspecimen aged at 1023K

was accomplished based on JCPDS card list. The XRD analysis has been performed on the specimens of conventional solution treatment as well as modified solution one. These XRD patterns exhibit the presence of γ matrix and MC carbides and disappearance of non-equilibrium phase, Ni_2Nb, in all specimens of conventional and modified solution specimens. The δ phase was found only in the conventional solution treatment specimens.

Figure 8(a) and 8(b) show the XDR patterns for the conventional and modified solution specimens after aging for 4 h at 1023K. The peaks of the γ′ and γ″ phases were not clear enough as well as for the presence of δ phase in the XRD pattern of conventional solution treatment specimen. Even after long aging time, 50h, at 1023K, the XRD patterns show the absence of δ phase in modified solution specimen.

Actually the identification of precipitated phases such as γ, γ″ and δ was a little bit complicated by using XRD and not as expected. Therefore, TEM was used in this research to confirm the identification of the precipitated phases.

TEM observations

Figure 9 shows the bright field image of the modified solution specimen, in which there is no observation for γ′ and γ″ phases. The bright field micrograph for the modified solution specimen that aged at 1023K for 8h is shown in figure 10(a) which indicates some precipitations of γ and γ″. The hardness value of modified

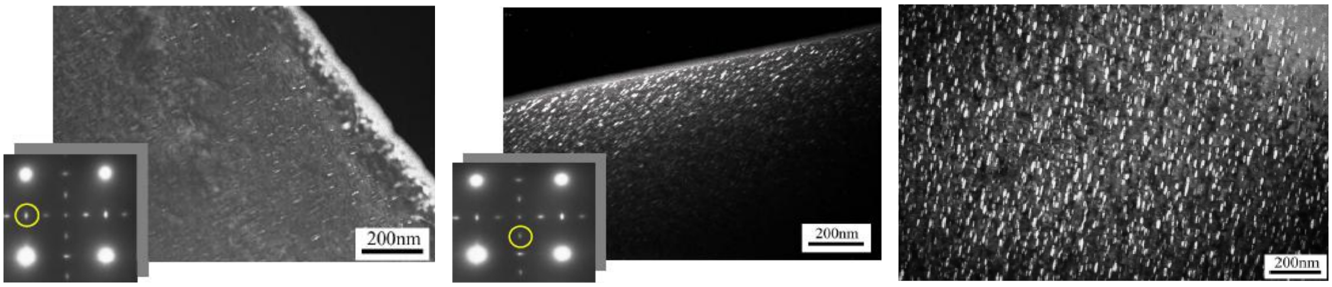

(a) (b) (c)

Figure 11 : Modified solution specimen aged at 1023K for 24h: (a) Dark field micrograph using (010) γ′ spot, (b) Dark field micrograph using (1 ½ 0) γ″ spot, (c) Dark field micrograph using (220) γ′ spot

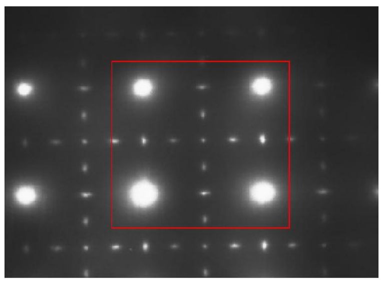

(a)

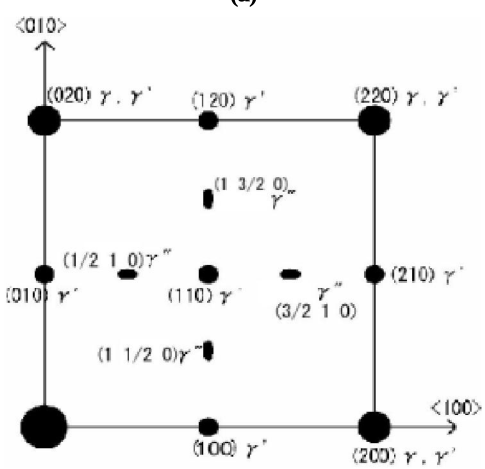

(b)

Figure 12 : The diffraction pattern of modified solution specimen aged at 1023k for 50h obtained from {100} matrix zone axis[22]

solution specimen after aging for 8h at 1023K is low (165Hv), as shown in figure 7(b) and it could be due to lower volume fraction of γ′ and γ″[23].

By prolonging the aging time to 24h at the same temperature, 1023K, the hardness value significantly increased to reach ≅ 390Hv as shown in figure 7(b). This increment should be directly related to the higher volume fraction of γ′ and γ″ precipitates. The bright field micrograph for the modified solution specimen aged at 1023K for 24h, figure 10(b) shows the precipitates of γ″ phase in the γ matrix. Figure 11(a) shows the dark field micrograph for γ′ precipitates in the modified solution specimen after aging at 1023K for 24h, obtained from (010) γ′ spot, and the precipitates are recognized to appear like spherical particles. Figure 11(b) shows the dark field micrograph obtained from the (1 ½ 0) γ″ spot, which usually appears as long disk–shaped, uniformly distributed in the matrix with a high density. Additionally, figure 11(c) illustrates the dark field micrograph obtained from the (220) γ′ spot.

As the aging time increased to 50h at 1023K, the visibility of the precipitates is enhanced. Figure 12(a) shows the <001> matrix zone axis selected area diffraction (SAD) pattern for the modified solution specimen aged for 50h at 1023K. Figure 12(b) demonstrates the key to SAD pattern, {100} and {110} type reflections correspond to both γ′ and γ″ phases whereas {1 ½ 0} type reflections correspond to only γ″. At these conditions of heat treatment the hardness value gets slightly increased to ≅ 400Hv. Figure 13(a) and 13(b) reveal the dark field micrograph obtained from (110) γ′ spot and (1 ½ 0) γ″ spot.

Although the δ phase is thermodynamically more stable than the γ″ phase, the sluggishness of the δ phase precipitation means that its formation up to about 1173K is always preceded by γ″ precipitations[24].

CONCLUSIONS

In this research two types of solution heat treatment, followed by the same aging conditions, were carried out for standard HIPed Inconel 718 alloy. Based on the results, the following conclusions could be drawn:

1 After aging at 953K, the hardness increases rapidly in case of standard solution (1273K for 1h) specimens than that for modified solution (1440K for 3h) specimens. After 100h, the hardness reached the same value for both standard and modified solu-

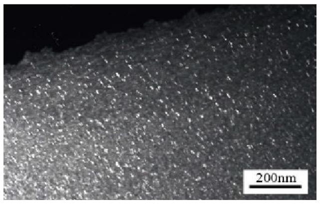

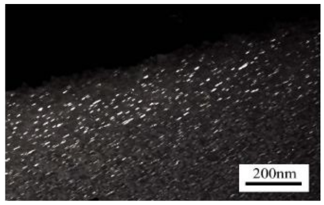

(a) (b)

Figure 13 : Modified solution specimen aged at 1023K for 50h: (a) Dark field micrograph using (010) γ' spot, (b) Dark field micrograph using (1 ½ 0) γ'' spot

tion specimens.

2 In case of aging at 1023K with short aging times (0-4h), the hardness for modified solution treated specimens need an incubation period to increase suddenly after 24h. While the hardness for conventional solution treated specimens increased dramatically with high acceleration with aging time. The hardness values for both conventional and modified solution treated specimens became nearly the same and increased slightly together after aging time for 24h.

3 By using EPMA, the microstructure of standard solution treated specimen revealed the precipitation of δ phase as a thin layer distributed at the grain boundaries and also as needle-like. While the microstructure for modified solution treated one shows no precipitation of δ phase neither at the grain boundaries nor as needle shape in the matrix.

4 After 100h aging at 1023K, SBSE and RE images confirmed the disappearing of δ phase from the microstructure of modified solution treated specimen.

5 As the aging time increases from 4h to 50h at 1023K, the colonies of the needle-like δ phase is enlarged and spread in the matrix. Prolonging the aging time increases the volume fraction of δ phase in conventional solution treated specimen.

REFERENCES

[1] T.Antonsson, H.Fredriksson; Metallurgical and Materials Transactions, B, **36(1)**, **(2005)**.

[2] A.Kermanpur, D.G.Evans, R.J.Siddall, P.D.Lee, M.McLean; Journal of Materials Science, **39(24)**, **(2004)**.

[3] K.R.Vishwakarma, N.L.Richards, M.C.Chaturvedi; Materials Science and Engineering, A, **480**, 517 **(2008)**.

[4] S.J.Hong, W.P.Chen, T.W.Wang; Metallurgical and Materials Transactions, A, **32(8)**, **(2001)**.

[5] T.S.Byun, K.Farrell; Journal of Nuclear Materials, 292 **(2003)**.

[6] Julien Deleume, Jean-Marc Cloue, Eric Andrieu; Journal of Nuclear Materials, **382**, 70 **(2008)**.

[7] Changzheng Wang, Rongbin Li; Journal of Materials Science, **39(7)**, **(2004)**.

[8] S.H.Fu, J.X.Dong, M.C.Zhang, X.S.Xie; Journal of Materials Science and Engineering, A, 215 **(2009)**.

[9] W.E.Quist, R.Taggart, D.H.Polonis; Met.Trans., **2**, 825 **(1971)**.

[10] S.Azdian, L.Y.Wei, F.Nicklasson, R.Warren; 'Precipitations in Spray-Formed IN 718', In: E.A.Loria, Editor; Superalloys 718, 625 and Various Derivatives, Warrendale, PA: Minerals, Metals, & Materials Society, 617 **(2001)**.

[11] Li Rongbin, He Xianchang, Yao Mei, Liu Wenchang; Journal of Materials Engineering and Performance, **11(5)**, **(2002)**.

[12] Yi Huang, G.Terence Langdon; Journal of Materials Science, **42(2)**, **(2007)**.

[13] Y.Desvallees, M.Bouzidi, F.Bois, N.Beaude; In: 'Superalloys 718, 625, 706 and Various Derivatives', Ed., E.A.Loria; 281 **(1994)**.

[14] M.Sundararaman, P.Mukhopadhyay, S.Banerjee; Metall.Trans.A, **19**, 453 **(1988)**.

[15] D.N.Duhl; 'Directionally Solidified Superalloys', In: C.T.Sims, N.S.Stoloff, W.C.Hagel, (Eds.); Superalloys 2, Wiley and Sins, Inc., New York, 189 **(1987)**.

[16] G.Appa Rao, M.Sirinivas, D.S.Sarma; Materials Science and Technology, **20**, 1161 **(2004)**.

[17] W.C.Liu, F.R.Xiao, M.Yao, Z.L.Chen, Z.O.Jiang, S.G.Wang; Scripta Materialia, **37(1)**, 59 **(1997)**.

[18] C.Salama, M.Abdellaoui; Journal of Alloys and Compounds, **306**, 277 **(2000)**.

[19] Saied Azadian, Liu-Ying Wei, Richard Warren; Materials Characterization, **53**, 7 **(2004)**.

[20] S.J.Hong, W.P.Chen, T.W.Wang; Metallurgical and Materials Transactions, A, **23**, 1887 **(2001)**.

[21] O.Lu Haz; 'Microstructural Evolution in Alloy 718 after Multiple Repair and PWHT Cycles', Ph.D. Thesis, Ohio State University, Ohio, United States, **(1999)**.

[22] C.M.Kuo, Y.T.Yang, H.Y.Bor, C.N.Wei, C.C.Tai; Materials Science and Engineering, A, **(2008)**.

[23] A.Strondl, R.Fischer, G.Frommeyer, A.Schnieder; Materials Science and Engineering, A, **480**, 138 **(2008)**.

[24] V.Beaubois, J.Huez, S.Coste, O.Brucelle, J.Lacaze; Materials Science and Technology, **20**, 1019 **(2004)**.